

### Germline biallelic *PIK3CG* mutations in a multifaceted immunodeficiency with immune dysregulation

The PI3K-AKT-mTOR signaling axis is a critical molecular pathway in humans, regulating multiple cellular processes.<sup>1</sup> Phosphatidylinositol-3-kinases (PI3K) represent key signaling hubs for signal propagation, driving cell activation, cell polarization and morphological adaptations. Studies on PI3K in human disease have highlighted PI3K-gamma (PI3K $\gamma$ ) as an appealing drug target for treatment of human disorders.<sup>2</sup> Murine PI3K $\gamma$  studies showed its importance in regulating innate immune functions and development<sup>3-4</sup> and activation of T cells,<sup>5</sup> revealing its role in controlling inflammation.<sup>4</sup> However, its role in the human immune system and diseases remains to be investigated.

Here we investigated a 14-year old female index patient, born to non-consanguineous healthy Austrian parents, who was hospitalized with severe hypotonia and prolonged fever. She had neither lymphadenopathy nor hepatosplenomegaly, and no infectious agent was found. Initial laboratory findings showed a mild thrombocytopenia, hypertriglyceridemia, increased lactate dehydrogenase (LDH) and markedly elevated ferritin (Table 1 and Figure 1A), prompting work up for hemophagocytic lymphohistiocytosis (HLH). Hemophagocytosis was indeed visible in the bone marrow aspirate (Figure 1B). Soluble CD25 was mildly elevated at 2204 U mL<sup>-1</sup> (Table 1) but below the levels typically seen in HLH.<sup>6</sup> NK-cell activity as measured by CD107a expression upon stimulation was in the low normal range in the initial diagnostic (Table 1). The presence of fever, hypertriglyceridemia, hyperferritinemia and hemophagocytosis, did not allow the diagnosis of HLH, but gave evidence of macrophage activation in the context of a hyperferritinemic inflammatory syndrome (Table 1).<sup>6</sup> We initiated treatment with dexamethasone, leading to clinical improvement and normalization of LDH and ferritin levels. Tapering of dexamethasone resulted in clinical deterioration and rise in ferritin (Figure 1A), and was accompanied by the development of autoimmune neutropenia as documented by HNA-1b antibodies. As the disease was distinct from classical HLH,<sup>6</sup> we decided to treat the patient with recombinant human anti-IL-1 $\beta$  (Anakinra, 100 mg twice daily) in combination with dexamethasone, rather than using the etoposide-based HLH-94 protocol. We discontinued dexamethasone treatment after eight weeks and, one month later, reduced the Anakinra dose to a maintenance dose of 100 mg daily. The patient has remained clinically stable and is currently receiving Anakinra (decreased to 60 mg once daily) without any inflammatory manifestations. Immunological characterization of patient peripheral blood in the asymptomatic phase after ceasing dexamethasone revealed reduced absolute natural killer (NK)-cell counts and low frequency of monocytes, and slightly low absolute lymphocyte counts (Table 1).

To explore a potential genetic etiology of the disease, we performed whole exome sequencing on patient DNA. We identified compound heterozygous variants in *PIK3CG* encoding for p110 $\gamma$ , the catalytic subunit of the PI3K $\gamma$  complex. Variants were validated by Sanger sequencing and both parents were identified as heterozygous carriers, each for one of the two variants (Figure 1C). The patient inherited a variant within the adaptor binding domain of p110 $\gamma$  (c.145C>A, p.R49S) and (c.3254A>G, p.N1085S) near the end of the kinase

domain (Figure 1D). Both variants are rare or absent in ExAC and gnomAD databases (*Online Supplementary Table S1*), and affect evolutionarily conserved residues (*Online Supplementary Figure S1A*). Probability of loss-of-function tolerance was unlikely, CADD and PolyPhen-2 scoring suggested the variants as probably pathogenic/damaging (*Online Supplementary Table S1*). We assessed the expression of mutated p110 $\gamma$  in T cells derived from patient peripheral blood mononuclear cells (PBMC), and found comparable expression levels in the patient, mother, and healthy donors (HD) (Figure 1E).

To investigate whether the identified *PIK3CG* mutations potentially cause the HLH-like disease due to defects in PI3K $\gamma$ -dependent mechanisms, we first studied patient-derived NK- and T-cell functions. Diminished NK-cell function is part of the diagnostic criteria for HLH.<sup>6</sup> *Pik3cg*<sup>-/-</sup> mice display reduced NK-cell numbers, defective NK-cell development and, consequently, decreased cytotoxicity.<sup>3</sup> We also observed reduced frequency, absolute counts and degranulation of patient NK cells compared to cells derived from the mother and HD (Table 1 and *Online Supplementary Figure S1B and C*). The impaired NK-cell compartment may have contributed to the observed clinical HLH-like phenotype.<sup>3</sup>

We further hypothesized that a defect in PI3K $\gamma$  signaling would affect TCR-driven activation of T cells.<sup>7</sup> Patient T-cell subsets were comparable to HD (*Online Supplementary Table S2*). However, we observed functional defects in patient T cells, particularly a poor activation and proliferation in response to anti-CD3 or combined anti-CD3/CD28 stimulation (Figure 2A and B and *Online Supplementary Figure S1D*). As expected, TCR-dependent T-cell activation was impaired in *PIK3CG*-mutated T cells. In contrast, patient T-cell proliferation was intact upon stimulation with phytohemagglutinin P (PHA) (Figure 2A and *Online Supplementary Figure S1D*) which can be explained due to the bypassing of TCR/PI3K $\gamma$ -dependent activation mechanisms. To prove the causative role of mutated *PIK3CG* for the observed phenotypes, we performed a gene-rescue experiment on primary patient cells using GFP-labeled wild-type p110 $\gamma$  and showed that the T-cell activation defect could be restored (Figure 2C). Additionally, we utilized the PI3K $\gamma$  inhibitor IPI-549 to prove the causative role of PI3K $\gamma$  loss-of-function for the observed phenotypes. T-cell activation and proliferation defects upon TCR stimulation were phenocopied by the addition of IPI-549 to HD cells (Figure 2D and E). Furthermore, we examined PI3K/AKT signaling and found mildly decreased AKT phosphorylation in patient cells upon stimulation (Figure 2F and *Online Supplementary Figure S1E*), similar to a recently reported patient with *PIK3CG* mutations.<sup>8</sup> To prove causality in an independent cellular system, we created Jurkat *PIK3CG* knockout (KO) cells (*Online Supplementary Figure S1F*) and found decreased activation as measured by CD69 upregulation upon anti-CD3 stimulation (Figure 2G), and reduced AKT phosphorylation at the Ser473 phosphorylation site (Figure 2H and *Online Supplementary Figure S1F and G*). These data mimic the phenotypes observed in patient T cells. Furthermore, upon reconstitution with wild-type p110 $\gamma$ , CD69 was upregulated on the surface of Jurkat *PIK3CG* KO cells (*Online Supplementary Figure S1H*). By contrast, upon reconstitution of mutant N1085S or R49S, no upregulation of CD69 was observed compared to empty vector (*Online Supplementary Figure S1H*), showing loss-of-function mechanisms for both individual variants. Altogether, the T-cell stimulation defects observed in *PIK3CG*-mutated patient cells recapitulate reports on *Pik3 $\gamma$* <sup>-/-</sup> murine T cells.<sup>5,7</sup>

For the development of familial HLH, absence of the cytotoxic activity of cytotoxic T cells (CTL) plays a central role. The level of surface CD107a/LAMP1 was normal on patient CTL upon stimulation (*Online Supplementary Figure S4I*). Furthermore, consistent with

murine studies suggesting that PTEN activity, counteracting PI3K function, is required to maintain Treg cell stability and homeostasis,<sup>9</sup> we observed a slightly increased frequency of CD4<sup>+</sup>CD127<sup>dim</sup>FOXP3<sup>+</sup>CD25<sup>+</sup>T<sub>reg</sub> cells in the peripheral blood of the patient (*Online Supplementary*

**Table 1.** Patient's immunological features.

Features	Initial presentation (July 2018)	After ceasing dexamethasone (Dec 2018)	After reducing Anakinra (June 2019)
Hb (g/dL)	12.3 (12.3-16)	12.6 (12.3-16)	13.1 (12.3-16)
Absolute lymphocytes (x10 <sup>9</sup> /L)	<b>0.95</b> (1.1-4.5)	<b>1.07</b> (1.1-4.5)	<b>0.95</b> (1.1-4.5)
Absolute neutrophils (x10 <sup>9</sup> /L)	3.48 (1.9-8.0)	1.95 (1.9-8.0)	<b>1.05</b> (1.9-8.0)
Absolute monocytes (x10 <sup>9</sup> /L)	0.24 (0.15-1.4)	0.15 (0.15-1.4)	0.15 (0.15-1.4)
CD3 <sup>+</sup> CD16 <sup>+</sup> CD14 <sup>+</sup> monocytes (%)	NA	<b>7.59</b> (24.1-11.8)	NA
Absolute thrombocytes (x10 <sup>9</sup> /L)	<b>119</b> (140-400)	334 (140-400)	296 (140-400)
Absolute CD3 <sup>+</sup> T cells (x10 <sup>9</sup> /L)	<b>0.71</b> (0.75-2.51)	0.99 (0.75-2.51)	0.75 (0.75-2.51)
Absolute CD4 <sup>+</sup> T cells (x10 <sup>9</sup> /L)	<b>0.37</b> (0.43-1.69)	0.53 (0.43-1.69)	0.43 (0.43-1.69)
Absolute CD8 <sup>+</sup> T cells (x10 <sup>9</sup> /L)	0.3 (0.22-1.21)	0.4 (0.22-1.21)	0.28 (0.22-1.21)
Absolute CD56 <sup>+</sup> CD3 <sup>-</sup> NK cells (x10 <sup>9</sup> /L)	<b>0.06</b> (0.12 - 0.60)	<b>0.06</b> (0.12 - 0.60)	<b>0.07</b> (0.12 - 0.60)
Absolute CD19 <sup>+</sup> B cells (x10 <sup>9</sup> /L)	0.13 (0.12-0.64)	<b>0.09</b> (0.12-0.64)	<b>0.08</b> (0.12-0.64)
HLH determinants [criteria for familial HLH]			
Ferritin (ng/mL) [>500]	<b>13898</b> (7-150)	33 (7-150)	22 (7-150)
Fibrinogen (mg/dL) [<150]	242 (150-450)	236 (150-450)	NA
Triglycerides (mg/dL) [>265]	<b>265</b> (0-150)	41 (0-150)	NA
NK-cell degranulation <sup>†</sup> [low/absent]	10.64 (>10)	NA	NA
sCD25 (U/mL) [>2400]	<b>2204</b> (158-623)	<b>1320</b> (158-623)	NA
IgG (g/L)	11 (4.9-16.1)	6.16 (6-16)	NA
IgM (g/L)	1.27 (0.5-1.9)	<b>0.28</b> (0.5-1.9)	NA
IgA (g/L)	0.98 (0.4-2.0)	<b>0.27</b> (0.8-2.8)	NA
HiB IgG (µg/mL)	8.15	1.46	NA
Diphtheria IgG (IU/mL)	0.15	0.05	NA
Tetanus IgG (IU/mL)	1.25	0.25	NA

Reference ranges are indicated in round brackets. Values out of reference ranges are indicated in bold. Criteria ranges for familial HLH<sup>6</sup> are indicated in squared brackets. Hb: hemoglobin; HiB: *Haemophilus influenzae* B antibody; HLH: hemophagocytic lymphohistiocytosis; Ig: immunoglobulin; NA: not applicable; sCD25: soluble CD25; <sup>†</sup>%CD107<sup>+</sup> cells, according to the standard diagnostic measurement conducted at the Centre for Chronic Immunodeficiency, University of Freiburg, Freiburg, Germany.

Figure S1J). In comparison to T cells which activate *via* PI3K $\gamma$  and PI3K $\delta$ , B cells predominantly respond *via* PI3K $\delta$ . This was corroborated by impaired B-cell development compared to rather intact T-cell populations in *PIK3CD* and *PIK3R1* loss-of-function patients.<sup>10</sup> By contrast, *PIK3CG*-mutated patient-derived B cells showed intact proliferation and class switch recombination upon stimulation (Online Supplementary Figure S1K and L), supporting data obtained in *Pik3cg*<sup>-/-</sup> mice.<sup>5</sup>

Since PI3K $\gamma$  is highly expressed in myeloid cells, we hypothesized that loss-of-function mutations in human PI3K $\gamma$  may compromise the function of these cells, thereby potentially contributing to the inflammatory features reported in the patient. Indeed, the observation that the patient responded well to anti-IL-1 $\beta$  (Anakinra) therapy (Figure 1A) supports the notion that defects in the PI3K pathway in innate immune cells may underlie the inflammatory presentation. Preclinical studies have shown that PI3K $\gamma$  blockade leads to reprogramming of macrophages, resulting in increased production of pro-inflammatory cytokines.<sup>11</sup> PI3K $\gamma$  activation results in the PIP<sub>3</sub>-dependent activation of Rac and, subsequently, Arp2/3-dependent actin-cytoskeleton remodeling driving cell polarization, morphology and phagocytosis.<sup>12</sup> We hypothesized that

*PIK3CG*-mutated patient cells would display abnormalities in innate cell morphology and function. We therefore differentiated freshly-isolated monocytes of patient, mother and HD to macrophages, which showed comparable expression of macrophage differentiation markers (Online Supplementary Figure S2A), implying normal differentiation. Upon stimulation, the number of adhered cells per image was similar across all groups (Online Supplementary Figure S2B). However, patient monocyte-derived macrophages displayed dramatic reduction in cell area and total amount of F-actin per cell, as compared to HD cells (Figure 2I-K). Moreover, cells from the mother displayed an intermediate phenotype, possibly linked to her heterozygous carrier status for one of the *PIK3CG* mutations. Altogether, these data indicate that PI3K $\gamma$  deficiency is associated with a defect in actin-driven macrophage spreading upon stimulation. We also observed diminished phagocytosis in patient-derived monocytes and neutrophils (Figure 2L). Patient neutrophils showed a pronounced apoptotic population after isolation (Online Supplementary Figure S2C). Loss of mitochondrial membrane potential in neutrophils is an early marker for commitment to apoptosis.<sup>13</sup> Consistently, mitochondrial membrane potential of patient neutrophils

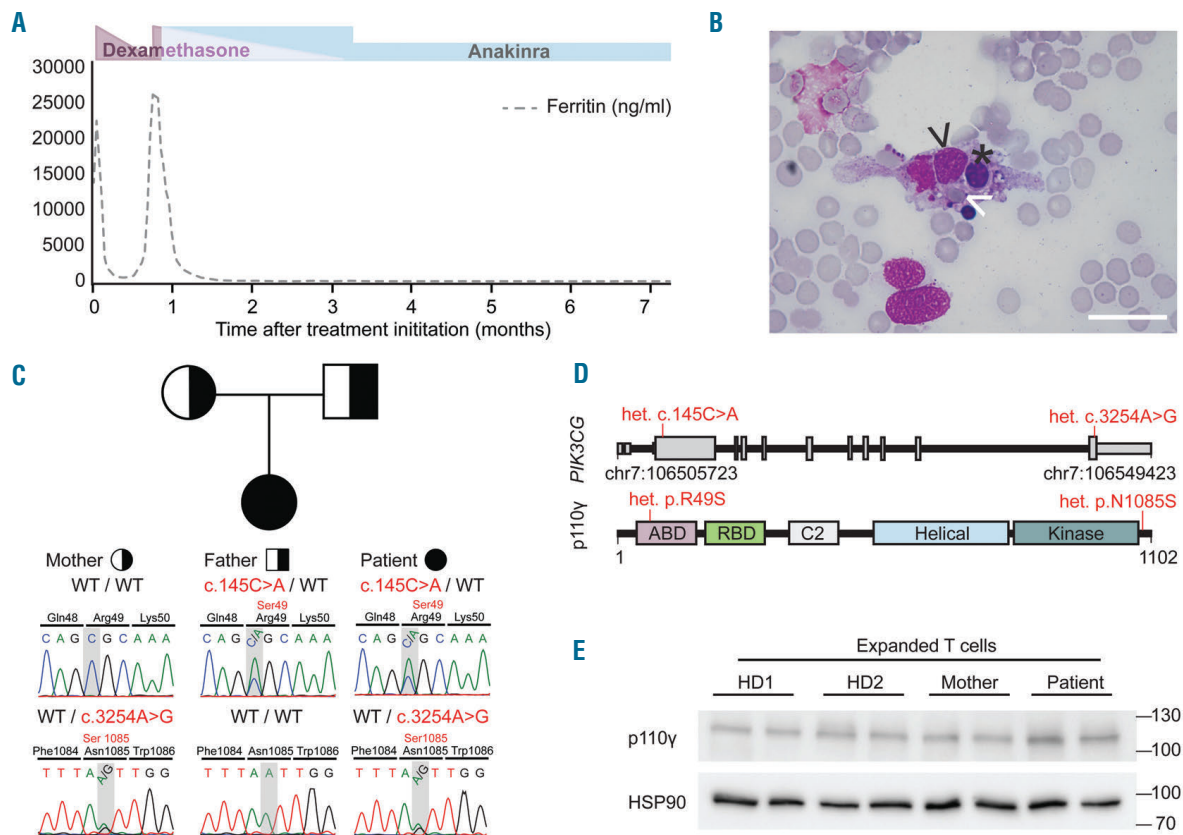


**Figure 1. Compound-heterozygous *PIK3CG* mutations in a patient with systemic inflammation.** (A) Patient response to dexamethasone treatment (purple) as evidenced by the decrease of ferritin in the patient's peripheral blood. Disease relapsed upon initial withdrawal of dexamethasone, as evidenced by increased ferritin levels. Reinitiation of dexamethasone normalized ferritin levels, and treatment with Anakinra (blue) was initiated and well-tolerated. Treatment was initiated at 14 years of age, and ferritin was monitored over seven months. Colored bars indicate drug dosage. (B) Patient bone marrow biopsy showing engulfment of erythroblast (black asterisk) and mature erythrocyte (white arrow) by a macrophage. The nucleus is indicated by the black arrow. Scale bar: 25  $\mu$ m. (C) Compound-heterozygous *PIK3CG* base pair substitutions in the index patient (filled symbol) segregate with parents. Sanger sequencing confirmed presence of a heterozygous variant in each parent (half-filled symbols). (D) Schematic representation of chromosomal position (top) and protein domains (bottom) of the identified *PIK3CG*/p110 $\gamma$  mutations, introducing two distinct missense mutations within the adaptor-binding domain (ABD) and near the kinase domain of the protein (bottom). RBD: Ras-binding domain; het: heterozygous. (E) Expression of p110 $\gamma$  protein in expanded T cells of the patient, compared with cells of mother and two healthy donors (HD). HSP90 was used as a housekeeping loading control.

was compromised (*Online Supplementary Figure S2D*). However, patient neutrophils displayed a normal oxidative burst upon stimulation (*Online Supplementary Figure S2E*). Studies in mice outlined the importance of PI3K $\gamma$  in neutrophils.<sup>14</sup> However, in a transwell migration assay,

patient neutrophils were able to migrate normally (*Online Supplementary Figure S2F*). Since PI3K $\delta$  works synergistically with PI3K $\gamma$  in neutrophil migration, PI3K $\delta$  may compensate for migration processes in human neutrophils. Collectively, we report deficiency of human

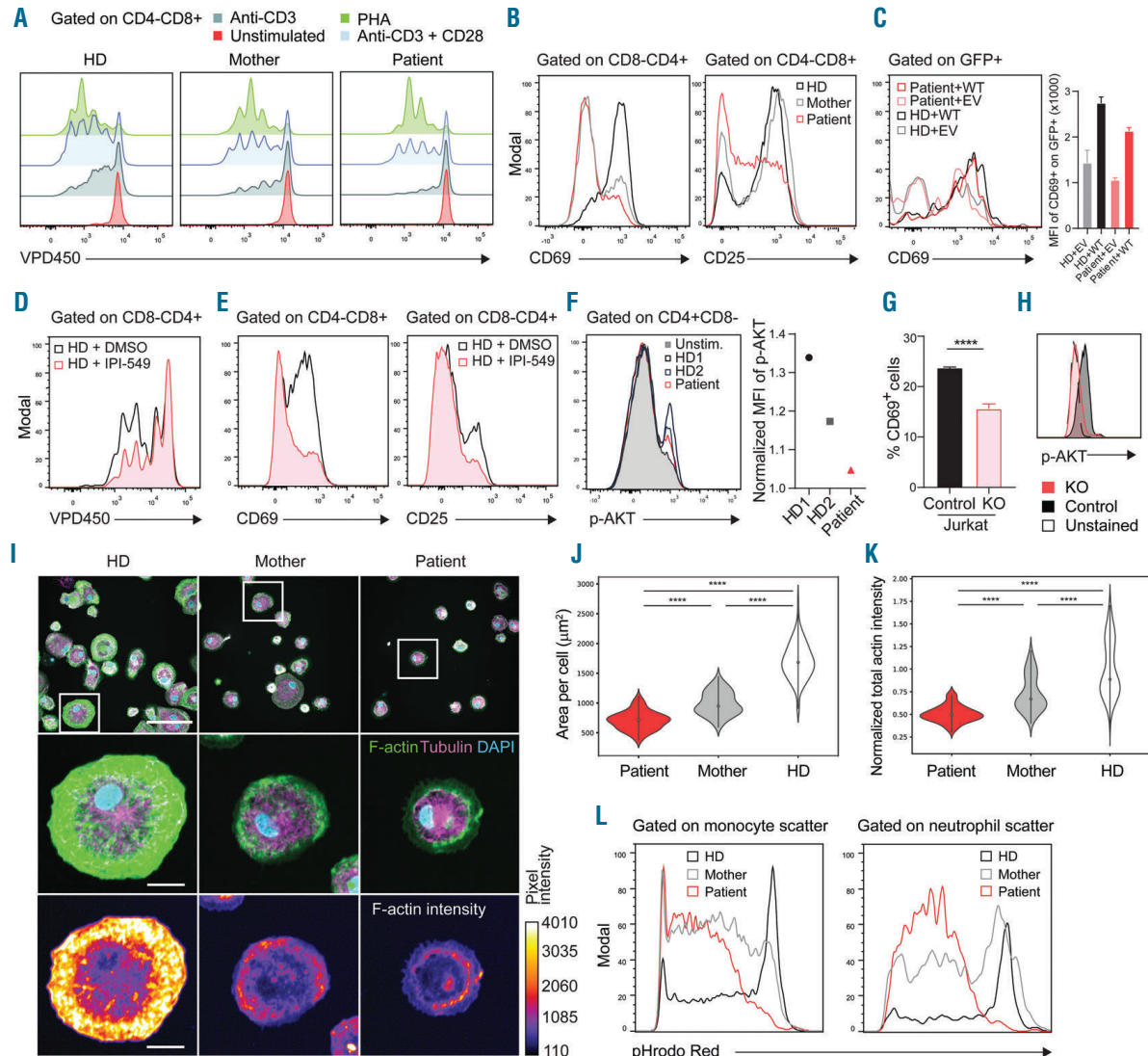


**Figure 2.** *PI3K3CG* mutations affect adaptive and innate immune functions. (A) Reduced proliferative capacity of patient-derived T cells upon stimulation with anti-CD3 antibody or combined anti-CD3/CD28 antibody. Phytohemagglutinin P (PHA) stimulation was not impaired, in agreement with TCR/PI3K-independent T-cell activation. Cells were stained with violet proliferation dye (VPD450), and dye dilutions were monitored three days post stimulation. (B) Impaired activation of patient T cells. Peripheral blood mononuclear cells (PBMC) were isolated and stained for the appearance of activation markers, one day (left, CD69 upregulation) or three days (right, CD25 upregulation) after stimulation with anti-CD3/CD28. Cells were gated on lymphocytes and CD8<sup>+</sup>CD4<sup>+</sup> (left) or CD4<sup>+</sup>CD8<sup>+</sup> (right) populations. (C) Rescue of T-cell activation via CD69 expression on day 2 post stimulation with anti-CD3 in patient cells by exogenous expression of wild-type (WT) *PI3K3CG* or empty vector (EV). Gated on GFP<sup>+</sup> transfected cells (left). Mean fluorescence intensity (MFI) of CD69 expression on GFP<sup>+</sup> transfected cells (right). (D) PI3K $\gamma$  inhibition by IPI-549 phenocopies T-cell proliferation defects. Cells were stimulated with anti-CD3/CD28 and monitored for VPD450 dye dilution as in (A). (E) Addition of PI3K $\gamma$  inhibitor IPI-549 (1  $\mu$ M) phenocopies the T-cell activation defect, compared to DMSO control. Cells were stimulated as in (B) and gated on CD4<sup>+</sup>CD8<sup>+</sup> (left) or CD8<sup>+</sup>CD4<sup>+</sup> (right) lymphocytes. (F) Impaired activation of AKT signaling in *PI3K3CG*-mutated patient PBMC, gated on CD4<sup>+</sup>CD8<sup>+</sup> T cells. PBMC were stimulated with anti-CD3/CD28 for 15 minutes. (Left) Phospho-AKT signal was reduced in patient cells compared to healthy donors (HD). (Right) Normalization to unstimulated control. (G) Decreased activation of *PI3K3CG* knockout (KO) Jurkat cells compared to Renilla KO control upon anti-CD3 stimulation. \*\*\*\* $P$ <0.0001, two-way ANOVA. (H) Reduced MFI of AKT Ser473 phosphorylation in *PI3K3CG* KO Jurkat cells compared to Renilla KO control and unstained control. (I) Representative immunostaining images of 40 $\times$  magnification after 5 hours incubation with PMA/ionomycin in HD, mother and patient monocyte-derived macrophages. Images show reduced cell spreading and total F-actin intensity in patient macrophages upon stimulation. Scale bars: 100  $\mu$ m (top), 20  $\mu$ m (middle, bottom). The lookup table (bottom right) indicates a color code for pixel values. (J) Patient macrophages show lack of cell spreading as indicated by significantly smaller cell area compared to mother and HD cells. \*\*\*\* $P$ <0.0001, Mann-Whitney  $U$  test. (K) Reduced total F-actin intensity of patient macrophages compared to mother and HD cells. \*\*\*\* $P$ <0.0001, Mann-Whitney  $U$  test. (L) Reduced phagocytosis ability of patient-derived monocytes (left) and neutrophils (right). Whole-blood samples were incubated with pHrodo Red *E. coli* and phagocytosed bacteria were evaluated by flow cytometry. Populations were gated based on forward/side scatter characteristics of monocytes and neutrophils, respectively. All error bars indicate  $\pm$  standard error of mean.

p110 $\gamma$  underlying a previously unknown inborn error of immunity with HLH-like systemic inflammation and aberrant immune cell function. Intriguingly, despite compromised functions of both innate and adaptive immune cells, so far the patient has not experienced serious infections as compared to a patient recently reported with PI3KCG mutations.<sup>8</sup> Larger patient cohorts and longer follow up will thus be necessary to unravel the full clinical spectrum of the disease.

Marini Thian,<sup>1,2,3,4</sup> Birgit Hoeger,<sup>1,2,3</sup> Anton Kamnev,<sup>1</sup> Fiona Poyer,<sup>5</sup> Sevgi Köstel Bal,<sup>1,2,3</sup> Michael Caldera,<sup>5</sup> Raúl Jiménez-Heredia,<sup>1,2,3</sup> Jakob Huemer,<sup>1,2,3</sup> Winfried F. Pickl,<sup>6</sup> Miriam Groß,<sup>7</sup> Stephan Ehl,<sup>7</sup> Carrie L. Lucas,<sup>8</sup> Jörg Menche,<sup>3</sup> Caroline Hutter,<sup>2,5</sup> Andishe Attarbaschi,<sup>5</sup> Loïc Dupré<sup>1,9</sup> and Kaan Boztug<sup>1,2,3,4,5</sup>

<sup>1</sup>Ludwig Boltzmann Institute for Rare and Undiagnosed Diseases, Vienna, Austria; <sup>2</sup>St. Anna Children's Cancer Research Institute (CCRI), Vienna, Austria; <sup>3</sup>CeMM Research Center for Molecular Medicine of the Austrian Academy of Sciences, Vienna, Austria; <sup>4</sup>Department of Pediatrics and Adolescent Medicine, Medical University of Vienna, Vienna, Austria; <sup>5</sup>St. Anna Children's Hospital, Department of Pediatrics and Adolescent Medicine, Medical University of Vienna, Vienna, Austria; <sup>6</sup>Institute of Immunology, Center for Pathophysiology, Infectiology and Immunology, Medical University of Vienna, Vienna, Austria; <sup>7</sup>Institute for Immunodeficiency, Center for Chronic Immunodeficiency (CCI), Medical Center - University of Freiburg, Faculty of Medicine, University of Freiburg, Freiburg, Germany; <sup>8</sup>Department of Immunobiology, Yale University School of Medicine, New Haven, CT, USA and <sup>9</sup>Center for Pathophysiology of Toulouse Purpan, INSERM UMR1043, CNRS UMR5282, Paul Sabatier University, Toulouse, France

**Funding:** this work was funded by the European Research Council (ERC Consolidator Grant 820074 to KB) and the Vienna Science and Technology Fund (WWTF-LS16-060 to KB and LD). MT was supported by the Cell Communication in Health and Disease programme (CCHD, Medical University of Vienna) and a DOC fellowship of the Austrian Academy of Sciences (ÖAW 25225). BH was supported by the Austrian Science Fund FWF Hertha Firnberg program (T934-B30). SE and MG were supported by the Deutsche Forschungsgemeinschaft SFB1160 (TPA01).

**Acknowledgments:** the authors thank the patient and her family for participating in this study. We thank Javier Rey-Barroso (Institute of Pharmacology and Structural Biology of Toulouse) for the excellent technical advice. We thank the Superti-Furga laboratory, especially

Felix Kartnig (CeMM), for technical assistance and access to the microscope. We thank Ana Krolo (LBI-RUD), Yolla German (LBI-RUD & Center for Pathophysiology of Toulouse Purpan), Arno Rottal and Ulrike Körmöcz (Institute of Immunology, Medical University of Vienna) for technical assistance.

Correspondence: KAAN BOZTUG - kaan.boztug@ccri.at

doi:10.3324/haematol.2019.231399

## References

1. Fruman DA, Chiu H, Hopkins BD, et al. The PI3K Pathway in Human Disease. *Cell*. 2017;170(4):605-635.
2. Janku F, Yap TA, Meric-Bernstam F. Targeting the PI3K pathway in cancer: are we making headway? *Nat Rev Clin Oncol*. 2018;15:273-291.
3. Tassi I, Cella M, Gilfillan S, et al. p110 $\gamma$  and p110 $\delta$  Phosphoinositide 3-Kinase Signaling Pathways Synergize to Control Development and Functions of Murine NK Cells. *Immunity*. 2007;27(2):214-227.
4. Kaneda MM, Messer KS, Ralainirina N, et al. PI3K $\gamma$  is a molecular switch that controls immune suppression. *Nature*. 2016; 539(7629):437-442.
5. Sasaki T, Irie-Sasaki J, Jones RG, et al. Function of PI3K $\gamma$  in Thymocyte Development, T Cell Activation, and Neutrophil Migration. *Science*. 2000;287(5455):1040-1046.
6. Henter J-I, Home A, Arico M, et al. HLH-2004: Diagnostic and therapeutic guidelines for hemophagocytic lymphohistiocytosis. *Pediatr Blood Cancer*. 2007;48(2):124-131.
7. Alcázar I, Marques M, Kumar A, et al. Phosphoinositide 3-kinase  $\gamma$  participates in T cell receptor-induced T cell activation. *J Exp Med*. 2007;204(12):2977-2987.
8. Takeda AJ, Maher TJ, Zhang Y, et al. Human PI3K $\gamma$  deficiency and its microbiota-dependent mouse model reveal immunodeficiency and tissue immunopathology. *Nat Commun*. 2019;10:4364-4376.
9. Huynh A, DuPage M, Priyadharshini B, et al. The phosphatase PTEN-mediated control of PI-3 kinase in Tregs cells maintains homeostasis and lineage stability. *Nat Immunol*. 2015;16(2):188-196.
10. Nunes-Santos C, Uzel G, Rosenzweig SD. PI3K pathway defects leading to immunodeficiency and immune dysregulation. *J Allergy Clin Immunol*. 2019;143(5):1676-1687.
11. De Henau O, Rausch M, Winkler D, et al. Therapy by targeting PI3K  $\gamma$  in myeloid cells. *Nature*. 2016;539(7629):443-447.
12. Hawkins PT, Stephens LR. PI3K signalling in inflammation. *Biochim Biophys Acta*. 2015;1851(6):882-897.
13. Fossati G, Moulding DA, Spiller DG, et al. The mitochondrial network of human neutrophils: role in chemotaxis, phagocytosis, respiratory burst activation, and commitment to apoptosis. *J Immunol*. 2003;170(4):1964-1972.
14. Hirsch E, Katanaev VL, Garlanda C, et al. Central Role for G Protein-Coupled Phosphoinositide 3-Kinase  $\gamma$  in Inflammation. *Science*. 2000;287(5455):1049-1054.